DOI:
10.2967/jnumed.114.148353

Document Version
Peer reviewed version

Journal of Nuclear Medicine, published on April 16, 2015 as doi:10.2967/jnumed.114.148353

^{64}CuCTS: a promising radiopharmaceutical for the identification of low grade cardiac hypoxia by PET

Rodolfo A Medina, Erika Mariotti, Davor Pavlovic*, Karen P Shaw, Thomas R Eykyn, Philip J Blower, Richard Southworth

King's College London, Division of Imaging Sciences & Biomedical Engineering, &

*Division of Cardiovascular Research,

The Rayne Institute.

St. Thomas' Hospital, London, UK

Corresponding author

Richard Southworth

Imaging Sciences & Biomedical Engineering, King's College London, St. Thomas' Hospital, Lambeth Palace Rd, London, SE1 7EH, UK

Tel: +44(207) 1888374

Fax: +44(207) 1885442

richard.southworth@kcl.ac.uk

Word count: 4923.

Running title: **^{64}CuCTS images low grade cardiac hypoxia**

Funder: British Heart Foundation

ABSTRACT

The subtle hypoxia underlying chronic cardiovascular disease is an attractive target for PET imaging, but the lead hypoxia imaging agents ^{64}CuATSM and ^{18}FMISO trapped only at extreme levels of hypoxia and hence are insufficiently sensitive for this purpose. We have therefore sought an analog of ^{64}CuATSM better suited to identify compromised but salvageable myocardium, validated using parallel biomarkers of cardiac energetics comparable to those observed in chronic cardiac ischemic syndromes.

Methods: Rat hearts were perfused with aerobic buffer for 20 min, followed by a range of hypoxic buffers (using a computer-controlled gas mixer) for 45 min. Contractility was monitored by intraventricular balloon, energetics by ^{31}P NMR spectroscopy, lactate and creatine kinase release spectrophotometrically, and HIF1α by Western blotting.

Results: We identify a key hypoxia threshold at a 30% buffer O_2 saturation which induces a stable and potentially survivable functional and energetic compromise: LV developed pressure was depressed by 20%, and cardiac phosphocreatine was depleted by 65.5 ± 14% ($p<0.05$ vs control), but ATP levels were maintained. Lactate release was elevated (0.21 ± 0.067 versus 0.056 ± 0.01 mmol/L/min, $p<0.05$), but not maximal (0.46 ± 0.117 mmol/L/min), indicating residual oxidative metabolic capacity. HIF1α was elevated, but not maximal. At this key threshold, ^{64}CuCTS selectively deposited significantly more ^{64}Cu than any other tracer we examined (61.8 ± 9.6% injected dose versus 29.4 ± 9.5% for ^{64}CuATSM $p<0.05$).

Conclusion: The hypoxic threshold which induced survivable metabolic and functional compromise was 30% O_2. At this threshold, only ^{64}CuCTS delivered a hypoxic:normoxic contrast of 3:1, and it therefore warrants in vivo evaluation for imaging chronic cardiac ischemic syndromes.

Keywords- Cardiac hypoxia, PET, NMR, bioenergetics, Cu-ATSM, bis(thiosemicarbazones)

INTRODUCTION

Hypoxia is a major factor in the pathology of cardiac ischemia. It is an important factor in the etiology of microvascular disease and cardiac hypertrophy, the prime determinant of the progression to heart failure, and the driver for compensatory angiogenesis [1-3]. In microvascular disease, while gross perfusion measured by MRI or scintigraphy may appear normal, the myocardium is hypoxically compromised at the cellular level [4]. This makes it an extremely difficult condition to diagnose, currently assigned by exclusion of other pathologies [5]. In hypertrophic myocardium, perfusion is also often "normal", but increased cell size, loss of t-tubules, and scar means that increased diffusion distances critically limit oxygen delivery to mitochondria [6, 7]. To accurately characterise these conditions, imaging disparities between supply and demand for blood flow (ischemia), or O_2 (hypoxia), would be a potentially more useful approach than measuring poor perfusion per se [8], but as yet, there are no methodologies sufficiently sensitive or specific for this purpose [9, 10].

The PET tracer ^{64}CuATSM (R_1=R_3=R_4=R_6=Me, R_2=R_5=H, Fig 1), exhibits rapid first pass uptake and fast clearance from normoxic tissues [11] and blood [12], and rapid retention in hypoxic tissues to generate excellent images of tissue hypoxia within minutes. Experimentally, tissue ^{64}Cu accumulation from ^{64}CuATSM has been demonstrated only in extreme models of acute hypoxia and ischemia in isolated perfused hearts, and in regionally occluded canine myocardium in vivo [13, 14], appearing to have a hypoxia-selective threshold of 1mm Hg or lower [11, 15]. While this degree of hypoxia is compatible with the survival and radio-resistance of cancer cells, for which it was designed, it is too severe for the long-term survival of cardiac myocytes (normal cardiac mitochondrial pO_2 is 10-35 mm Hg) [16]. In the one very small (seven patient) cardiac clinical trial that has been performed to date using ^{62}CuATSM, ^{62}Cu accumulation was only visualised in the myocardium of one patient with unstable angina, despite four of those patients exhibiting increased regional ^{18}FDG uptake [12]. Thus, while CuATSM can be used to selectively identify the

extreme acute hypoxia commonly induced in experimental models, it seems insufficiently sensitive to detect the subtle hypoxia characterising the chronic cardiac ischemic syndromes that are currently difficult to identify [9].

The fundamental challenge, therefore, is to identify complexes which deposit their radiocopper payload within the myocardium at less extreme levels of hypoxia where its biochemistry is perturbed, but remains potentially salvageable. We reason that this target hypoxia "threshold" would be the point where there remains a degree of metabolic flexibility: a compromised but functional capacity for oxidative metabolism, but with sufficient ATP turnover to maintain ionic homeostasis and cellular integrity [9]. We have therefore performed a series of hypoxia titrations in the isolated heart to determine where this threshold lies using a panel of biochemical and biophysical assays. We then use a recently developed gamma detection array [17] to identify analogs of ^{64}CuATSM exhibiting greater sensitivity to hypoxia at this more relevant threshold.

MATERIALS AND METHODS

Reagents and Animals

All reagents were purchased from Sigma unless otherwise stated. Gases were supplied by BOC. Desired gas mixtures (O_2/N_2/CO_2) were achieved using a GSM-3 gas mixer (CWE Inc).

Male Wistar rats (275-300 g, Harlan), fed ad libitum, were used for all experiments. Animal procedures were in accordance with the Animals (Scientific Procedures) Act UK (1986).

Experimental Protocol

^{64}Cu was produced and used to radiolabel 2,3-butanedione bis (thiosemicarbazone) (ATS), diacetyl-bis(N4-ethylthiosemicarbazone) (ATSE), 2,3-butanedione bis(N4-

methylthiosemicarbazone) (ATSM) and 2,3-pentanedione bis(thiosemicarbazone) (CTS) as previously described [17].

Rats (n = 6/group) were anesthetized with Sagatal (100 mg ip) and heparinized (200 IU ip), their hearts excised and cannulated in the Langendorff mode [18]. Hearts were perfused at constant flow (to simplify pharmacokinetic modeling) of 14 ml/min with a modified Krebs-Henseleit buffer (KHB) described previously [17], gassed with 95% O_2/5% CO_2 gas mixture, and contractile function was measured with a left ventricular balloon. Perfusion pressure was monitored by a pressure transducer in the arterial line. Hearts were paced at 300 beats/min throughout.

After 20 minutes, perfusate delivery was switched to a second reservoir containing KHB equilibrated with a gas mixture containing either 95%, 40%, 30%, 20%, 10% or 0% O_2, balanced with N_2 and 5% CO_2 (for pH buffering), delivered by a gas mixer. 1 ml aliquots of coronary effluent were collected at regular intervals, and analysed for lactate content (YSI 2300 STAT Plus™ lactate analyser) to identify the onset of anerobic glycolysis, and creatine kinase content to monitor tissue necrosis. At the end of each experiment, hearts were snap-frozen in liquid nitrogen prior to Western blotting for HIF1α.

^{31}P Magnetic Resonance Spectroscopic Analysis (MRS)

Hearts were cannulated and inserted into a 15 mm glass MRS tube which was then placed in a custom-built MRS probe, as previously described [19]. ^{31}P MRS spectra were acquired on a Bruker Avance III 9.4T spectrometer using a 15 mm ^{31}P/^{1}H birdcage coil [20]. Shimming was performed on the ^{1}H lineshape of water (FWHM < 20 Hz). ^{31}P spectra were acquired with a pulse-acquire sequence using a 60^{o} flip angle, repetition time of 3.8 s and 64 scans (4 minutes per spectrum). The peak area of each metabolite was normalized to that of phosphocreatine (PCr) during normoxia.

Profiling of Radiotracer Retention and Elution

In parallel groups of hearts, radiotracer uptake and pharmacokinetics were monitored using a custom built "triple gamma detector system" [17], consisting of three orthogonally positioned lead-shielded NaI detectors interrogating the arterial input line, the heart, and the venous outflow lines respectively, each connected to a modified GinaSTAR™ instant thin layer chromatography system (Raytest Ltd). 100 µl boluses containing 1 MBq radiotracer were injected into the arterial line after 10 minutes of normoxia, and 5 and 25 minutes of hypoxia. Time-activity curves generated by the GinaSTAR™ were imported into MATLAB® (MathWorks®). Data were decay-corrected and normalized to the maximum value of each group. Tissue retention was calculated as the residual activity in the heart 20 minutes post-injection as a percentage of the peak activity (% injected dose, %ID), as previously described [21].

Western Blotting

Hearts were homogenized in 10 ml of homogenization buffer / g tissue (100 mM Tris pH 7.4, 2 mM sodium vanadate, 5 mM sodium fluoride, 1 x protease inhibitor cocktail tablet / 50 ml, 4°C). Equal volumes of homogenate and 2 x sodium dodecyl sulphate sample buffer were mixed before being loaded and separated by molecular weight using SDS-PAGE on a 10% polyacrylamide gel. Proteins were transferred to PVDF membranes (0.45 µm; GE Healthcare) using semi-dry blotting (Biorad). Blots were incubated for 2 hours at room temperature with hypoxia inducible factor (HIF-1α) antibody (rat polyclonal 5 µg/ml; Abcam). After incubation with HRP-labeled secondary antibodies, blots were developed using enhanced chemiluminescence (Amersham Pharmacia Biotech), with GAPDH as a loading control. HIF-1α and GAPDH expression were quantified through film-scanning and densitometry using Quantity One software (Biorad), with HIF-1α normalized to GAPDH.

Statistical Analysis

Analyses were performed using GraphPad Prism® (GraphPad Software Inc). All values are expressed as the mean±SD. A paired t-test was used for all pair-wise comparisons, and one way ANOVA with the Bonferroni correction for multi-way comparisons. Dunnett's post analysis test was applied when multiple comparisons were made to a control group.

RESULTS

All tracers examined deposited increasing amounts of radiocopper in the myocardium with increasingly severe hypoxia (Fig 2). Hypoxia selectivity was apparent within 5 minutes of onset (Fig 2a), with significant ^{64}Cu retention in hearts injected with ^{64}CuCTS with KHB equilibrated with 30% O_2 (40.9 ± 4.6% ID versus 13.7 ± 3.1% pre-hypoxia $p<0.05$), with an EC_{50} value of 32.1% O_2. While the other tracers also exhibited hypoxia selectivity, they were less sensitive; ^{64}Cu ATSM and ^{64}Cu ATSE were only selective at the 20% O_2 threshold (31.3 ± 1.42 and 39.34% ID, EC_{50} values of 18.9 and 22.9% O_2 respectively), while ^{64}CuATS was only selective at the 10% O_2 threshold (34.7 ± 12.7% ID, EC_{50} 7.4% O_2). The same selectivities were evident after 25 minutes (Figure 2b), although the absolute amount of radiocopper deposition in each case was greater. ^{64}CuCTS was the only tracer to selectively deposit radiocopper in the heart at 30% O_2 (61.8 ± 9.6% versus 15.8 ± 3.8% ID in normoxic hearts ($p<0.05$), EC_{50} 32% O_2), and consistently more than ^{64}CuATSM under all hypoxic conditions. The selectivity profiles of ^{64}CuATSM, ^{64}CuATSE and ^{64}CuATS were largely similar (EC_{50} values of 25.2, 25.1 and 22.2% O_2 respectively), although ^{64}CuATS deposited significantly more ^{64}Cu than ^{64}CuATSM at 0% O_2 (78 ± 7.2% versus 63.4 ± 11.5; $p<0.05$).

The critical threshold for decreasing LVDP within 5 minutes was 20% O_2, (to 68 ± 14 mm Hg from a pre-hypoxia 145 ± 12 mm Hg; $p<0.05$, Fig 3a), although perfusion pressure and LVEDP were unaffected. Perfusion with 30% O_2 KHB elevated LVEDP above pre-ischemic values after 25 minutes (36 ± 8 versus 5 ± 3 mm Hg; $p<0.05$), while perfusion pressure was only elevated within this timeframe by completely anoxic KHB (112 ± 12 versus 73 ± 9 mm Hg; $p<0.05$).

Representative ^{31}P NMR spectra from a heart perfused with 0% O_2 KHB are shown in fig 4A. PCr was depleted by ~20 minutes of hypoxia, with a concomitant increase in inorganic phosphate (P_i). Sugar phosphates became apparent within 8 minutes, and by 25 minutes, ATP

levels were compromised. 30% O_2 KHB decreased cardiac PCr within 5 minutes (to 65.5 ± 14% of pre-hypoxia; $p<0.05$, Fig 4B), while PCr was only compromised by 40%O_2 after 25 minutes (to 43.4 ± 1.4%; $p<0.05$). ATP levels were unaffected by 30% O_2 KHB, but were depleted by 20% O_2 KHB (from 66.8 ± 20% to 41.8 ± 17%; $p<0.05$, Fig 4C); perfusion with more hypoxic buffers achieved no greater degree of ATP loss. Sugar and inorganic phosphates were not elevated by hypoxia after 5 minutes, but accumulated after 25 minutes perfusion with 20% O_2 (116 ± 37% versus 60 ± 18% and 49.8 ± 22.2% versus 13.8 ± 10.3% respectively; $p<0.05$). While lactate washout was evident after 25 minutes of perfusion with 30% O_2 KHB, (0.21 ± 0.07 versus 0.01 ± 0.02 nmol during normoxia; $p<0.05$ (Fig 5A), it increased further with 20% O_2 KHB to a near-maximal value of 0.46 ± 0.11 ($p<0.05$). There was no evidence of creatine kinase leakage in any experimental group (data not shown). HIF-1α:GAPDH expression was elevated after 25 minutes of 30% O_2 KHB (0.278 ± 0.064 versus normoxic 0.175 ± 0.047; $p<0.05$, Fig 5B), rising to a maximum of 0.61 ± 0.08 with 0% O_2 KHB.

DISCUSSION

We recently demonstrated that ^{64}CuCTS and its analog ^{64}CuATS exhibit significantly greater hypoxia selectivity than the current lead compound ^{64}CuATSM in hearts perfused with hypoxic (0% O_2) buffer [17]. While a promising first step in the screening process, the key to the progression of this class of compounds is to identify complexes selective for levels of hypoxia which correlate with survivable (and treatable) cardiac disease [9, 10]. The relative sensitivities of these complexes to pathophysiologically relevant degrees of cardiac hypoxia were unknown. In this study, we identify a key hypoxic threshold that induces the major hallmarks of compromised but salvageable myocardium, which are: depressed contractile function, compromised PCr levels (but stable ATP levels), elevated HIF-1α expression, and increased but not maximal lactate washout (indicating residual oxidative reserve). At this threshold, achieved by perfusion with KHB saturated with 30%O_2, we demonstrate that ^{64}CuCTS is the only complex among the four evaluated that provides a hypoxic:normoxic tissue contrast which would be exploitable for PET imaging [9].

Our approach, of identifying parallel biomarkers of biochemical compromise to correlate against tracer uptake circumvents the difficult problem of describing tracer uptake in terms of absolute (and potentially arbitrary) intracellular oxygen concentrations, which are not only difficult to determine, but would also vary in relevance dependent upon oxygen demand, cardiac workload, and experimental model [16]. It also allows an immediate bioenergetic interpretation of the relevance of increased cardiac tracer retention, which is arguably translatable from the Langendorff perfused heart to the clinical situation. While changes in cardiac energetics can be quantified by ^{31}P spectroscopic imaging in clinical MR systems, the technical capacity and infrastructure to do so is not widespread, requires significant expertise, long acquisition times, and results in images of poor spatial resolution. Correlating PET tracer uptake with these key changes in cardiac energetics could therefore provide the same biochemical insight as ^{31}P MR

spectroscopic imaging, but exploit a technically simpler imaging approach with significantly greater temporal and spatial resolution (typical voxel sizes for clinical ^{64}Cu PET are 65 mm^3 [22], compared to 560 mm^3 for ^{31}P MRI at 3T) [23].

We demonstrate that perfusion of hearts with 30% O_2 saturated KHB significantly depleted PCr, but was sufficient to maintain intracellular ATP and a degree of contractility. These characteristics mirror the reductions in PCr:ATP ratio previously demonstrated by ^{31}P MRS in patients with heart failure [24,25] and hypertrophic cardiomyopathy [26], and correlate with declining left ventricular ejection fraction and increased mortality [27]. While moderate depletion of cardiac ATP has also been observed in patients diagnosed with hypertrophied and failing myocardium [28], we used a less severe experimental threshold where PCr levels were compromised, but ATP levels were maintained to provide a more sensitive means of screening for diagnostically relevant hypoxia-selective complexes. Crucially, while 30% O_2 KHB increased lactate release by the heart, the rate of lactate washout only became maximal when hearts were perfused with KHB equilibrated with 20% O_2 and below, suggesting that at 30% O_2 there was still an aerobic metabolic reserve. At this key threshold, therefore, cardiac energetics and contractile function were compromised, but there was residual oxidative metabolism (and by inference mitochondrial function), suggesting that this degree of hypoxia would be sustainable chronically, making it a reasonable model of chronic cardiac ischemia.

30% O_2 was also the threshold for increased intracellular HIF-1α. As the key regulator of hypoxic gene expression, HIF-1α is responsible for numerous acute and chronic adaptive responses to tissue hypoxia, ranging from elevated glucose uptake and altered calcium handling to cardiac remodelling [29], cardiomyopathy [30], microvascular disease [31] and heart failure [32], while chronic activation of HIF-1α in animal models leads to progressive heart failure and premature death [33]. Elevated HIF-1α was therefore a prerequisite for the threshold against which to evaluate our tracers. There is currently no non-invasive method for measuring

intracellular HIF-1α; a hypoxia-specific imaging agent which correlates with the onset of hypoxia-dependent HIF-1α stabilization, such as we identify in ^{64}CuCTS, is therefore a potentially useful development.

While our isolated heart model is ideal for establishing basic structure-activity relationships of new tracers, it is limited in that it cannot inform upon other important pharmacokinetic factors like tracer metabolism. Hueting et al. have recently suggested in this Journal that the biodistribution and pharmacokinetics of ^{64}Cu-acetate in tumour-bearing mice is similar to that of ^{64}Cu-ATSM when assessed after 2 or 16 hours, and that ^{64}Cu-acetate exhibits hypoxia selectivity in cultured cancer cells, suggesting that Cu-bis(thiosemicarbazone) complexes dissociate quickly *in vivo*, and that the resultant biodistribution observed by PET is that of free copper, questioning the validity of ^{64}CuATSM as a hypoxia tracer [34]. We and other groups have observed no such non-specific uptake up of ionic $^{64}Cu^{2+}$ salts in normoxic or hypoxic myocytes in culture [15], CHO cells [35], or in isolated buffer perfused hearts [17, 21]. The wide variation in pharmacokinetics and early biodistributions that the different bis(thiosemicarbazones) have been shown to display, with some being hypoxia selective (ATSM, ATS, CTS etc.) and some not (PTSM, GTSM), some crossing the blood-brain barrier (GTSM, PTSM, ATSM etc.) and some not (ATS)[36,37], would also argue against a common non-selective mechanism of early tissue uptake. If such a mechanism does exist, it is likely dependent on tracer metabolism, and late recirculation of $^{64}Cu^{2+}$ in copper transport proteins. We have recently shown that ^{64}CuATSM, ^{64}CuCTS and ^{64}CuATS all rapidly wash out of normoxic myocardium in rats in vivo to a stable low level within 5 minutes of injection, with no secondary “creep” of non-specific cardiac accumulation due to recirculation in the ensuing 30 minutes of imaging [17], and no significant ^{64}Cu retention in healthy myocardium by biodistribution after 90 minutes. If secondary recirculation of ^{64}Cu occurs at later time points, the time between injection and imaging, and the relative in vivo stability of these complexes would be an important consideration in their use and

interpretation. Our study and many others which precede it [14, 17, 21] highlight the rapid hypoxia selectivity and tissue clearance of these tracers (within 5 minutes from normoxic myocardium both ex vivo, and in vivo)[17, 38]. We would therefore suggest that the rapid kinetics of these tracers should be exploited to minimise the potential impact of metabolism and recirculation by keeping imaging times short.

We have used ^{64}Cu in these experiments because its 12 hour half life allows us to perform several experiments from each batch. However, its half life is not ideal in terms of patient exposure, and with a positron yield of only 17.8%, nor is its dosimetry. In contrast, ^{62}Cu production does not require a cyclotron, has a half life of only 9.74 min and a 98% positron yield. The rapid kinetics that these tracers display would be very well suited to exploiting the dose-limiting advantages of ^{62}Cu radiolabelling clinically. We have employed isolated perfused hearts in this study because the model allows the accurate and reproducible induction of a range of hypoxic severity which would not be possible (or survivable or measurable) in vivo. It should of course be noted that tracer pharmacokinetics may be different in blood than in aqueous solution, and that the relationship between cardiac workload, arterial blood supply and tracer retention are likely to differ from that in vivo. We have, however, demonstrated the relative hypoxia selectivities of these tracers perfused under the same conditions, and ^{64}CuCTS appears to be a significant improvement upon ^{64}CuATSM in terms of hypoxia sensitivity.

We are currently unable to explain fully why ^{64}CuCTS exhibits better selectivity for low grade hypoxia than ^{64}CuATSM. Previous reports have suggested that hypoxia selectivity might be primarily governed by redox potential, yet CuATS, CuCTS, CuATSM and CuATSE all have the same redox potential (-0.59V versus Ag/AgCl[35]) and different hypoxia selectivities. It therefore appears that while redox potential imparts hypoxia selectivity generally (the non-hypoxia selective tracer CuPTSM has a lower redox potential of -0.51V), subtle modification of redox

potential is not the only route by which hypoxia selectivity can be fine tuned. We previously demonstrated that decreasing tracer lipophilicity increased tracer fast clearance rate, and improved hypoxic/normoxic contrast over CuATSM[17] (the logP values of CuATSE, CuATSM, CuCTS and CuATS are 2.34, 1.61, 1.01 and 0.35 respectively [21, 35]). There is a limit to this tactic, however, since CuATS, which has the lowest lipophilicity, provided no further gain in hypoxia sensitivity at the 30% threshold. We speculate that the subtle balance between redox potential, lipophilicity and steric hindrance of redox and ligand exchange reactions governs residence time in the cell (and/or its intracellular localisation), and determine the rate at which each complex is reduced, reoxidised and dissociated to release its payload.

CONCLUSION

Hypoxia imaging has the capacity to augment current techniques for identifying viable but at-risk myocardium. Diffuse hypoperfusion associated with non-compensated hypertrophy or microvascular disease is currently difficult to diagnose by imaging perfusion; specifically imaging the resultant hypoxia by PET may be a useful alternative approach. While ^{64}CuATSM seems insufficiently sensitive to target myocardium compromised by such low- level survivable hypoxia, we identify ^{64}CuCTS as a potentially more suitable PET tracer in this regard.

ACKNOWLEDGEMENTS

The authors acknowledge financial support from the KCL BHF Centre of Research Excellence, BHF award RE/08/003 (project grant PG/10/20/28211), the Department of Health via the National Institute for Health Research (NIHR) comprehensive Biomedical Research Centre award to Guy's & St Thomas' NHS Foundation Trust in partnership with King's College London and King's College Hospital NHS Foundation Trust, and the King's College London and UCL Comprehensive Cancer Imaging Centre. Funded by the CRUK and EPSRC in association with the MRC and DoH (England). The views expressed are those of the authors and not necessarily those of the NHS, the NIHR or the Department of Health.

DISCLOSURES

None

REFERENCES

1. Giordano FJ. Oxygen, oxidative stress, hypoxia, and heart failure. *J. Clin. Invest.* 2005;115:500-508.

2. Essop MF. Cardiac metabolic adaptations in response to chronic hypoxia. *J. Physiol.* 2007;584:715-726.

3. Sabbah HN, Sharov VG, Goldstein S. Cell death, tissue hypoxia and the progression of heart failure. *Heart Fail. Rev.* 2000;5:131-138.

4. Lanza GA, Crea F. Primary coronary microvascular dysfunction: clinical presentation, pathophysiology, and management. *Circulation.* 2010;121:2317-2325.

5. Leung DY, Leung M. Significance and assessment of coronary microvascular dysfunction. *Heart.* 2011;97:587-595.

6. Des Tombe AL, Van Beek-Harmsen BJ, Lee-De Groot MBE, Van Der Laarse WJ. Calibrated histochemistry applied to oxygen supply and demand in hypertrophied rat myocardium. *Microsc. Res. Tech.* 2002;58:412-420.

7. Chung Y. Oxygen reperfusion is limited in the postischemic hypertrophic myocardium. *Am. J. Physiol.* 2006;290:H2075-H2084.

8. De Boer RA, Pinto YM, Van Veldhuisen DJ. The imbalance between oxygen demand and supply as a potential mechanism in the pathophysiology of heart failure: the role of microvascular growth and abnormalities. *Microcirculation.* 2003;10:113 - 126.

9. Handley MG, Medina RA, Nagel E, Blower PJ, Southworth R. PET imaging of cardiac hypoxia: Opportunities and challenges. *J. Mol. Cell. Cardiol.* 2011;51:640-650.

10. Sinusas AJ. The potential of myocardial imaging with hypoxia markers. *Semin Nucl Med.* 1999;29:330-338.

11. Dearling J, Lewis J, Mullen G, Welch M, Blower P. Copper bis(thiosemicarbazone) complexes as hypoxia imaging agents: structure-activity relationships. *J. Biol. Inorg. Chem.* 2002;7:249-259.

12. Takahashi N, Fujibayashi Y, Yonekura Y, et al. Copper-62 ATSM as a hypoxic tissue tracer in myocardial ischemia. *Ann. Nucl. Med.* 2001;15:293-296.

13. Lewis JS, Laforest R, Buettner TL, et al. Copper-64-diacetyl-bis(N4-methylthiosemicarbazone): an agent for radiotherapy. *PNAS.* 2001;98:1206-1211.

14. Fujibayashi Y, Cutler CS, Anderson CJ, et al. Comparative studies of Cu-64-ATSM and C-11-acetate in an acute myocardial infarction model: ex vivo imaging of hypoxia in rats. *Nucl. Med. Biol.* 1999;26:117-121.

15. Handley MG, Medina RA, Paul RL, Blower PJ, Southworth R. Demonstration of the retention of 64Cu-ATSM in cardiac myocytes using a novel incubation chamber for screening hypoxia-dependent radiotracers. *Nucl Med Comms.* 2013;34:1015-1022.

16. Mik EG, Ince C, Eerbeek O, et al. Mitochondrial oxygen tension within the heart. *J. Mol. Cell. Cardiol.* 2009;46:943-951.

17. Handley MG, Medina RA, Mariotti E, et al. Cardiac hypoxia imaging: second generation analogues of 64Cu-ATSM. *J. Nucl. Med.* 2014;55:488-494.

18. Southworth R, Garlick PB. Dobutamine responsiveness, PET mismatch, and lack of necrosis in low-flow ischemia: is this hibernation in the isolated rat heart? *Am J Physiol.* 2003;285:H316-324.

19. Weiss K, Mariotti E, Hill D, et al. Developing Hyperpolarized ^{13}C Spectroscopy and imaging for metabolic studies in the isolated perfused rat heart. *Appl. Magn. Res.* 2012;43:275-288.

20. Garlick PB, Medina RA, Southworth R, Marsden PK. Differential uptake of FDG and DG during post-ischaemic reperfusion in the isolated, perfused rat heart. *Eur J Nucl Med.* 1999;26:1353-1358.

21. Fujibayashi Y, Taniuchi H, Yonekura Y, Ohtani H, Konishi J, Yokoyama A. Copper-62-ATSM: a new hypoxia imaging agent with high membrane permeability and low redox potential. *J. Nucl. Med.* 1997;38:1155-1160.

22. Nyflot MJ, Harari PM, Yip S, Perlman SB, Jeraj R. Correlation of PET images of metabolism, proliferation and hypoxia to characterize tumor phenotype in patients with cancer of the oropharynx. *Radiother. Oncol.* 2012;105:36-40.

23. Tyler DJ, Emmanuel Y, Cochlin LE, et al. Reproducibility of ^{31}P cardiac magnetic resonance spectroscopy at 3 T. *NMR Biomed.* 2009;22:405-413.

24. Hardy CJ, Weiss RG, Bottomley PA, Gerstenblith G. Altered myocardial high-energy phosphate metabolites in patients with dilated cardiomyopathy. *Am. Heart J.* 1991;122:795-801.

25. Neubauer S, Krahe T, Schindler R, et al. ^{31}P magnetic resonance spectroscopy in dilated cardiomyopathy and coronary artery disease. Altered cardiac high-energy phosphate metabolism in heart failure. *Circulation.* 1992;86:1810-1818.

26. Hansch A, Rzanny R, Heyne JP, Leder U, Reichenbach JR, Kaiser WA. Noninvasive measurements of cardiac high-energy phosphate metabolites in dilated cardiomyopathy by using ^{31}P spectroscopic chemical shift imaging. *Eur Radiol.* 2005;15:319-323.

27. Neubauer S, Horn M, Cramer M, et al. Myocardial phosphocreatine-to-ATP ratio Is a predictor of mortality in patients with dilated cardiomyopathy. *Circulation.* 1997;96:2190-2196.

28. Beer M, Seyfarth T, Sandstede J, et al. Absolute concentrations of high-energy phosphate metabolites in normal, hypertrophied, and failing human myocardium measured noninvasively with ^{31}P-SLOOP magnetic resonance spectroscopy. *J. Am. Coll. Cardiol.* 2002;40:1267-1274.

29. Hölscher M, Schäfer K, Krull S, et al. Unfavourable consequences of chronic cardiac HIF-1α stabilization. *Cardiovasc. Res.* 2012.

30. Roura S, Planas F, Prat-Vidal C, et al. Idiopathic dilated cardiomyopathy exhibits defective vascularization and vessel formation. *Eur. J. Heart Fail.* 2007;9:995-1002.

31. Hoenig MR, Bianchi C, Rosenzweig A, Sellke FW. The cardiac microvasculature in hypertension, cardiac hypertrophy and diastolic heart failure. *Curr. Vasc. Pharmacol.* 2008;6:292-300.

32. Semenza GL. Hypoxia-inducible factor 1 and cardiovascular disease. *Annu. Rev. Physiol*. 76. 2014:39-56.

33. Lei L, Mason S, Liu D, et al. Hypoxia-inducible factor-dependent degeneration, failure, and malignant transformation of the heart in the absence of the Von Hippel-Lindau protein. *Mol Cell Biol.* 2008;28:3790-3803.

34. Hueting R, Kersemans V, Cornelissen B, et al. A comparison of the behavior of ^{64}Cu-acetate and ^{64}Cu-ATSM In vitro and in vivo. *J. Nucl. Med.* 2014;55:128-134.

35. Dearling JLJ, Lewis JS, Mullen GED, Rae MT, Zweit J, Blower PJ. Design of hypoxia-targeting radiopharmaceuticals: selective uptake of copper-64 complexes in hypoxic cells in vitro. *Eur. J. Nucl. Med. Mol. Imaging.* 1998;25:788-792.

36. Wallhaus TR, Lacy J, Whang J, Green MA, Nickles RJ, Stone CK. Human biodistribution and dosimetry of the PET perfusion agent copper-62-PTSM. *J. Nucl. Med.* 1998;39:1958-1964.

37. Green MA, Klippenstein DL, Tennison JR. Copper(II) bis(thiosemicarbazone) complexes as potential tracers for evaluation of cerebral and myocardial blood flow with PET. *J. Nucl. Med.* 1988;29:1549-1557.

38. Lewis JS, Herrero P, Sharp TL, et al. Delineation of hypoxia in canine myocardium using PET and copper(II)-diacetyl-bis(N4-methylthiosemicarbazone). *J. Nucl. Med.* 2002;43:1557-1569.

Figure 1

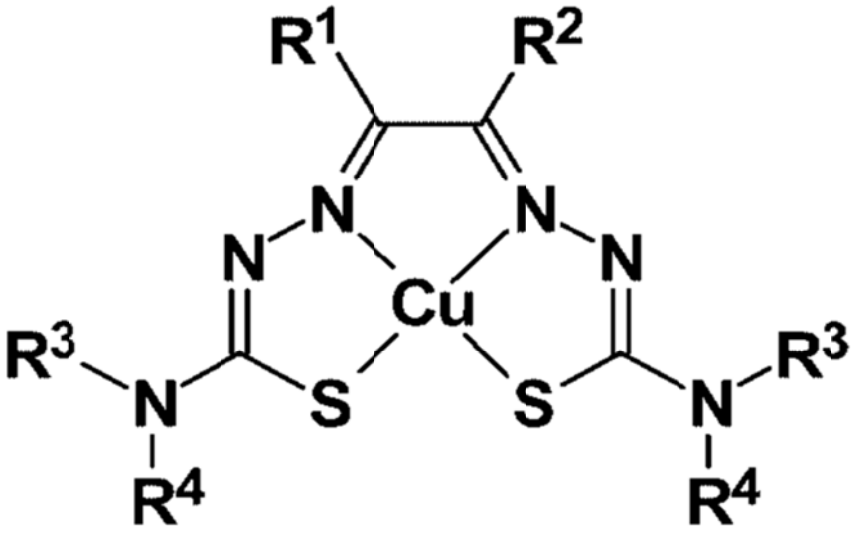

Figure 1: General structure of the bis(thiosemicarbazones). ^{64}CuATS: $R^1=R^2=CH_3$, $R^3=R^4=H$; ^{64}CuATSM=$R^1=R^2=R^3=CH_3$, $R^4=H$; ^{64}CuCTS=$R^1=C_2H_5$, $R^2=CH_3$, $R^3=R^4=H$; ^{64}CuATSE: $R^1=R^2=R^3=R^4=CH_3$

Figure 2

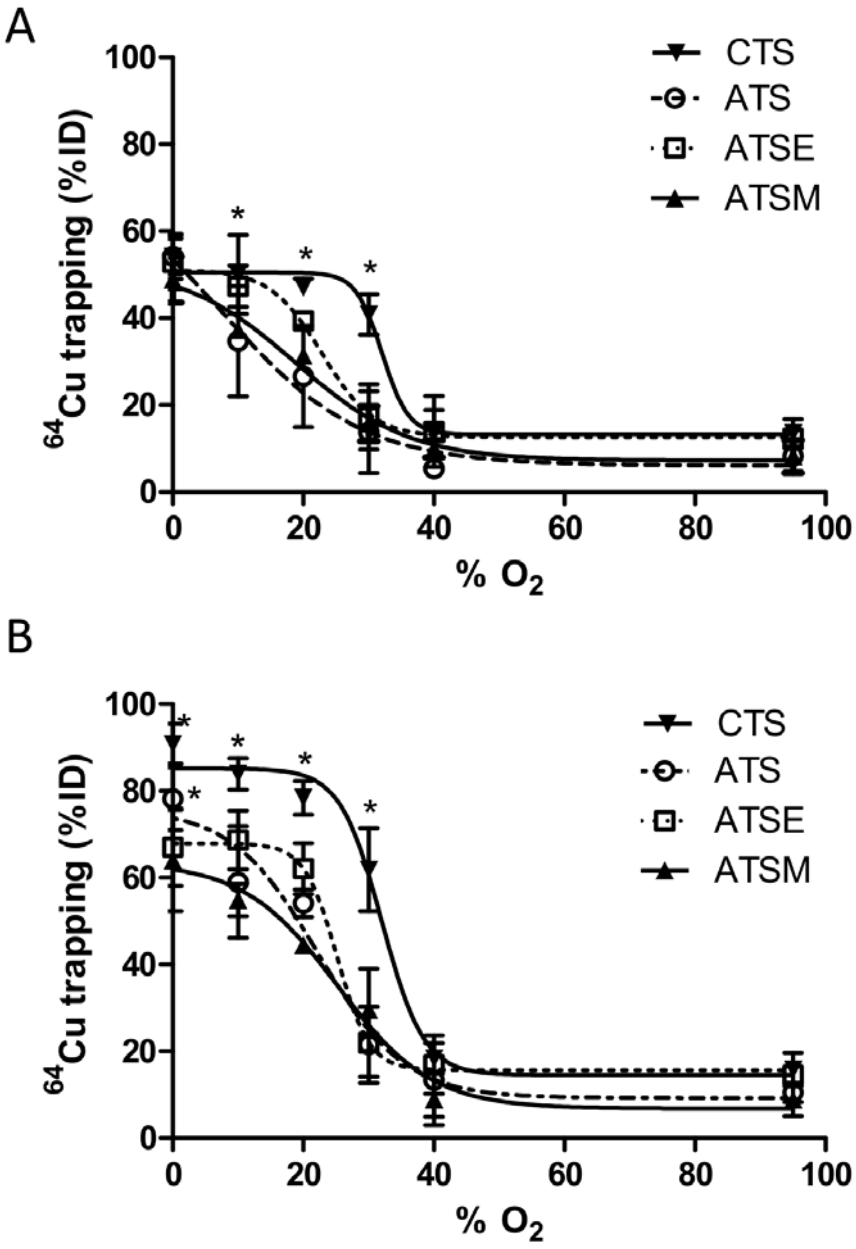

Figure 2: The relationship between hypoxic buffer perfusion and ^{64}Cu radiotracer uptake. Data (mean n=6±SD), represent cardiac ^{64}Cu retention from each tracer for ^{64}CuCTS (closed triangles), ^{64}CuATS (open circles), ^{64}CuATSE (open squares), and ^{64}CuATSM (closed triangles) as a percentage of injected dose 10 minutes after injection after (A) 5 minutes and (B) 25 minutes hypoxia. *significantly different from pre-hypoxic control values ($p<0.05$).

Figure 3

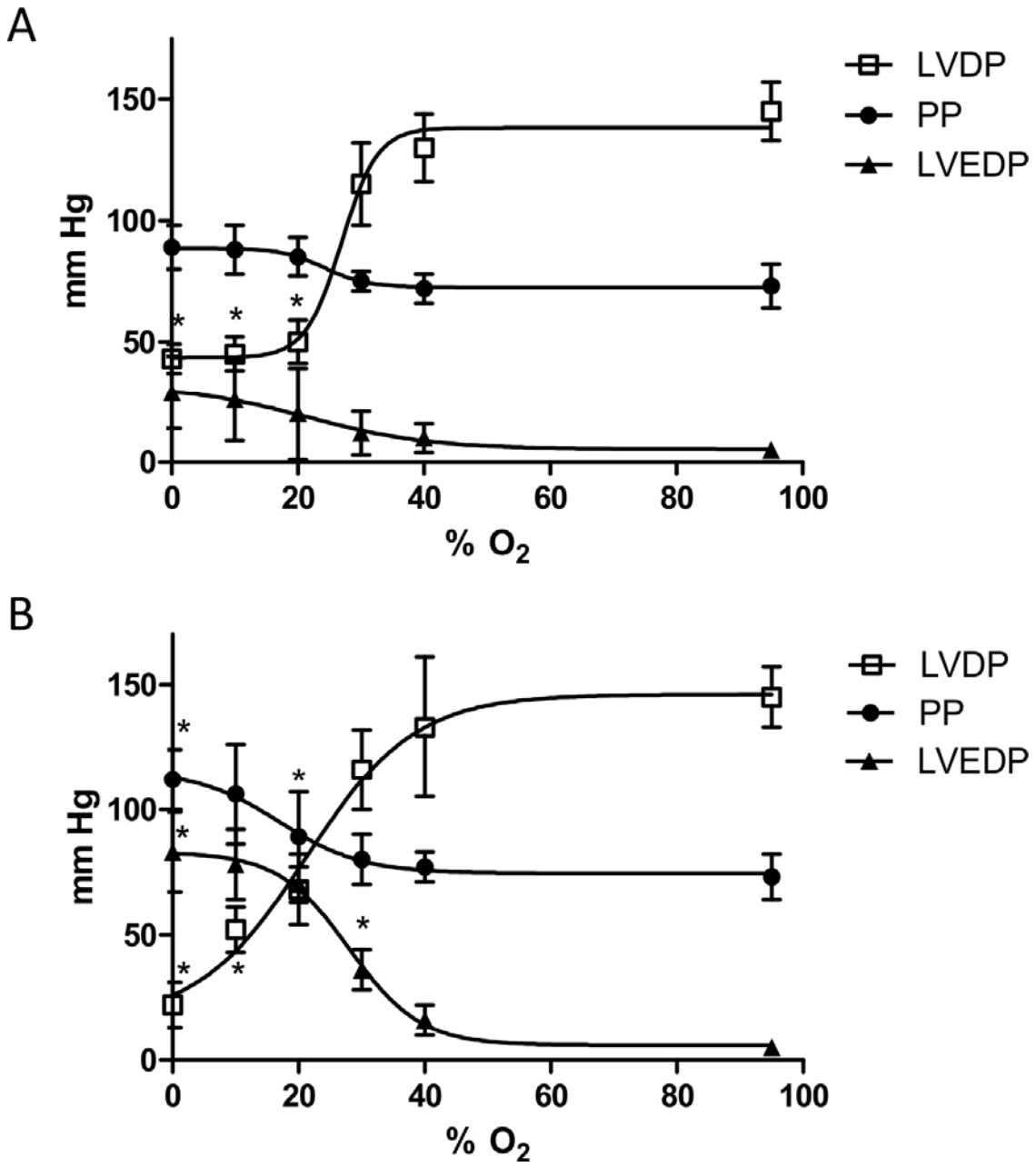

Figure 3: The relationship between hypoxic buffer perfusion and cardiac contractility and haemodynamics. Data (mean n=6±SD) represent changes in left ventricular developed pressure (LVDP), left ventricular end diastolic pressure (LVEDP) and perfusion pressure (PP), after (A) 5 minutes and (B) 25 minutes hypoxia. *significantly different from pre-hypoxic values ($p<0.05$).

Figure 4

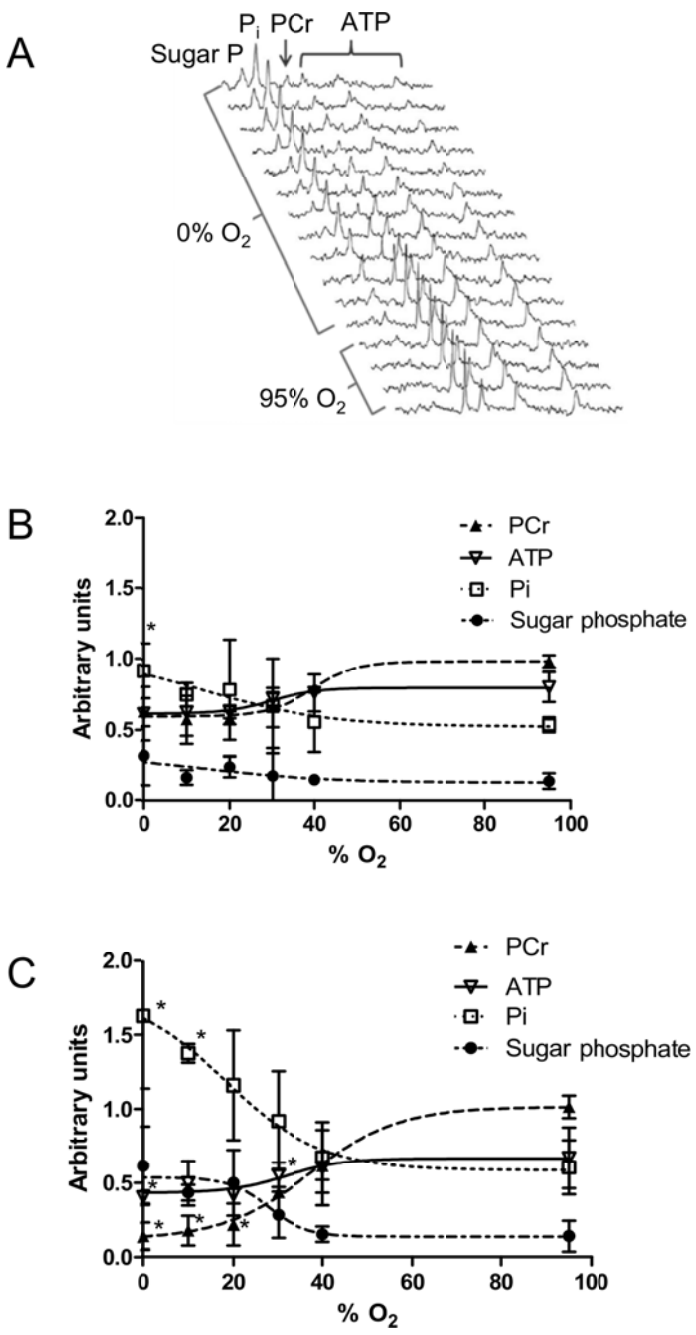

Figure 4: (A) Representative ^{31}P NMR spectra showing the changes in cardiac energetics during perfusion with 0% O_2 buffer. (B and C): The relationship between hypoxic buffer perfusion and cardiac energetics. Data mean (n=6±SD) represent changes in phosphocreatine (PCr, closed triangles), ATP (open triangles), inorganic phosphate (Pi, open squares), and sugar phosphates (closed circles) after 5 minutes and 25 minutes hypoxia. *significantly different from pre-hypoxic values ($p<0.05$).

Figure 5

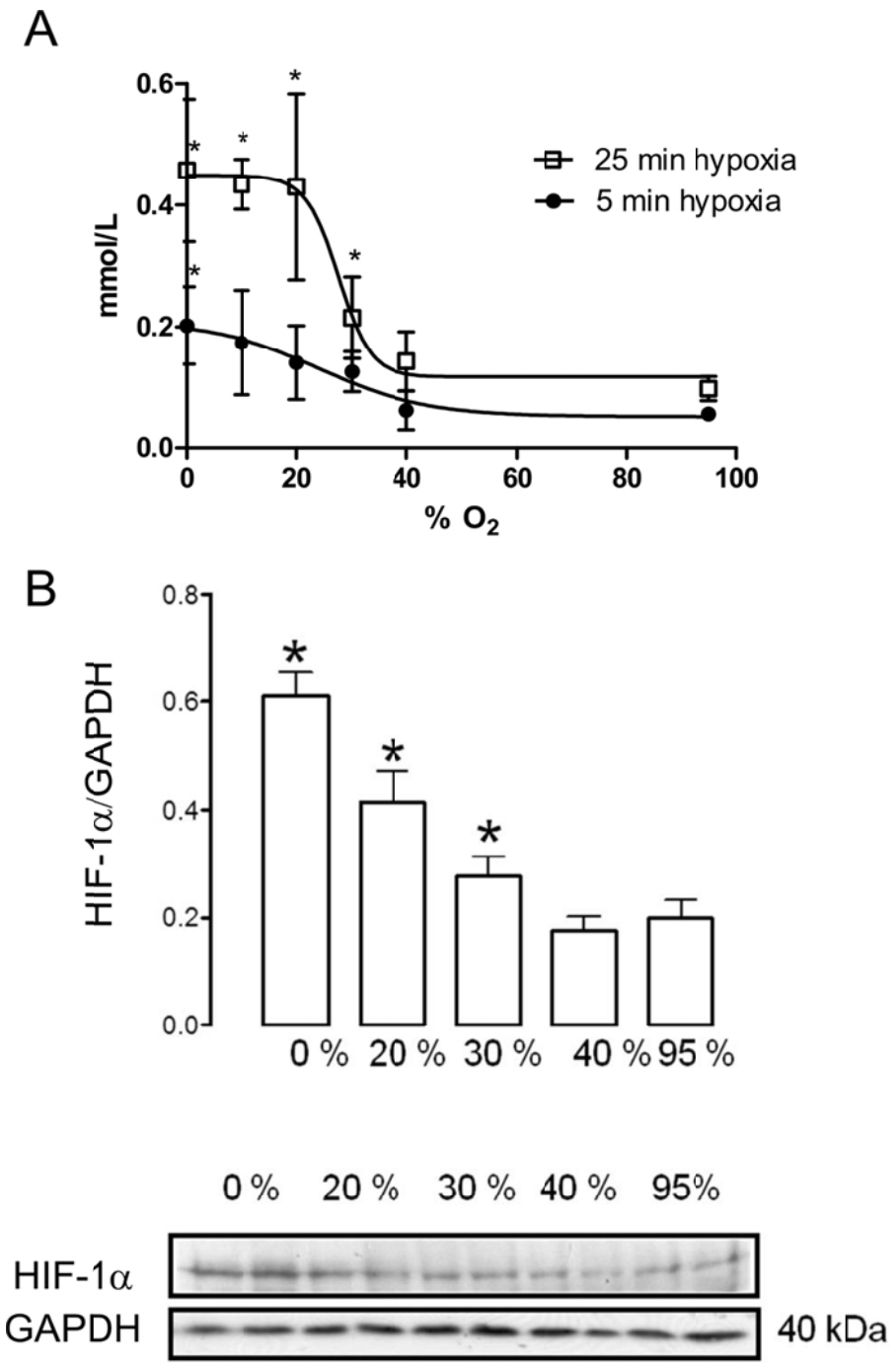

Figure 5: (A) The relationship between hypoxic buffer perfusion and lactate washout after 5 minutes (closed circles) and 25 minutes (open squares) of hypoxia, and (B) HIF1α expression at the end of each perfusion protocol. Data (mean n=6±SD), *significantly different from pre-hypoxic values ($p<0.05$).

The Journal of NUCLEAR MEDICINE

^{64}CuCTS: a promising radiopharmaceutical for the identification of low grade cardiac hypoxia by PET

Rodolfo Alfredo Medina, Erika Mariotti, Davor Pavlovic, Karen P Shaw, Thomas R Eykyn, Philip John Blower and Richard Southworth

J Nucl Med.
Published online: April 16, 2015.
Doi: 10.2967/jnumed.114.148353

The Journal of Nuclear Medicine is published monthly.
SNMMI | Society of Nuclear Medicine and Molecular Imaging
1850 Samuel Morse Drive, Reston, VA 20190.
(Print ISSN: 0161-5505, Online ISSN: 2159-662X)

SNMMI SOCIETY OF NUCLEAR MEDICINE AND MOLECULAR IMAGING